Advantages of a dual-color fluorescence-tracing glioma orthotopic implantation model: Detecting tumor location, angiogenesis, cellular fusion and the tumor microenvironment

YUNTIAN SHEN[1*], QUANBIN ZHANG[2*], JINSHI ZHANG[3], ZHAOHUI LU[1], AIDONG WANG[1], XIFENG FEI[4], XINGLIANG DAI[1], JINDING WU[1], ZHIMIN WANG[4], YAODONG ZHAO[2], YE TIAN[1], JUN DONG[1], QING LAN[1] and QIANG HUANG[1]

[1]Department of Neurosurgery, Radiotherapy and Oncology, The Second Affiliated Hospital of Soochow University, Suzhou, Jiangsu 215004; [2]Department of Neurosurgery, Shanghai Tenth People's Hospital, Shanghai 200072; [3]Department of Neurosurgery, Ganzhou People's Hospital, Ganzhou, Jiangxi 341000; [4]Department of Neurosurgery, Suzhou Kowloon Hospital, Suzhou, Jiangsu 215002, P.R. China

Received November 22, 2014; Accepted September 1, 2015

DOI: 10.3892/etm.2015.2821

Abstract. Various organs of the body have distinct microenvironments with diverse biological characteristics that can influence the growth of tumors within them. However, the mechanisms underlying the interactions between tumor and host cells are currently not well understood. In the present study, a dual-color fluorescence-tracing glioma orthotopic implantation model was developed, in which C6 rat glioma cells labeled with the red fluorescent dye CM-Dil, and SU3 human glioma cells stably expressing red fluorescence protein, were inoculated into the right caudate nucleus of transgenic female C57BL/6 nude mice expressing enhanced green fluorescent protein. The dual-color tracing with whole-body *in vivo* fluorescence imaging of xenografts was performed using a live imaging system. Frozen sections of the transplanted tumor were prepared for histological analyses, in order to detect the presence of invading tumor cells, blood vessels and cellular fusion. Dual-color images were able to distinguish between red tumor cells and green host cells. The results of the present study suggested that a dual-color fluorescence-tracing glioma orthotopic implantation model may be convenient for detecting tumor location, angiogenesis, cellular fusion, and the tumor microenvironment.

Correspondence to: Dr Jun Dong or Dr Qing Lan, Department of Neurosurgery, Radiotherapy and Oncology, The Second Affiliated Hospital of Soochow University, 1055 Sanxiang Road, Suzhou, Jiangsu 215004, P.R. China
E-mail: djdongjun@163.com
E-mail: szlq006@163.com

*Contributed equally

Key words: dual-color fluorescence, fluorescence-tracing, glioma, orthotopic implantation model, cellular fusion

Introduction

It is well known that genetic variation within the cells initiating a tumor leads to neoplasia; however, the tumor microenvironment theory suggests that host-derived components also participate in malignant tumor progression (1). It has previously been demonstrated that glioma stem progenitor cells have an important role in glioma tissue remodeling, and that host-derived components, including an altered vascular system, and glial cells that are transformed by glioma stem progenitor cells, may contribute substantially to tumor development (2,3). These results markedly improve the understanding of tumor-host interactions.

The earliest theory linking host-derived components with tumor progression was Paget's 'seed and soil' hypothesis (4), which proposed that tumor cells, or 'seeds', randomly disseminate within the blood flow, although they can only survive in permissive organs (i.e., the 'soil').

Fidler (5-7) further developed the 'seed and soil' hypothesis, and claimed that the tumor microenvironment is able to promote tumor growth. Furthermore, Fidler hypothesized that the biological characteristics of the microenvironments of various organs are distinct, and that the growth of metastatic cells depends on their interactions with host cells; however, the mechanisms underlying these interactions are not well understood, due to the lack of an appropriate animal model.

Hoffman developed a novel BALB/c nude mouse model that expressed green fluorescent protein (GFP), and subsequently established a red fluorescent protein (RFP)/GFP human cancer xenograft model by transplanting numerous solid tumor cells expressing RFP into the mice. These xenograft models permitted *in vivo* visualization and facilitated the study of host-tumor interactions in histological sections (8-11). Our previous study succeeded in cultivating two nude mouse strains, NC-C57BL6J-EGFP and BALB/c-C57BL6J-EGFP (12), which were subsequently used to study the efficacy of using dual-color fluorescence tracing in the investigation of glioma.

The present study compared dual-color fluorescence tracing with traditional methods in order to analyze tumor characteristics, including localization, angiogenesis, cellular fusion, and the tumor microenvironment. The dual-color fluorescence tracing method is seldom used to study brain tumors.

Materials and methods

Materials. The SU3 human glioma cell line was established in our laboratory. The C6 rat glioma cell line was obtained from the Institute of Biochemistry and Cell Biology Shanghai Institutes for Biological Sciences, Chinese Academy of Sciences (Shanghai, China). The CM-Dil dye was purchased from Invitrogen Life Technologies (Carlsbad, CA, USA) and the RFP lentiviral vector was purchased from Yingweixing Biological Science Technologies Co. (Shanghai, China). The nude NC-C57BL6J-EGFP and BALB/c-C57BL6J-EGFP mice (age, 6-8 weeks; weight, 22-24 g) were established and reared by our group in independent ventilation cages. The *in vivo* FX Pro Imaging system was purchased from Eastman Kodak (Rochester, NY, USA), and a fluorescence torch (DFP-1) was purchased from Nightsea (Lexington, MA, USA). The Eclipse TE2000U fluorescence inverted microscope was obtained from Nikon Corporation (Tokyo, Japan), and the BB16 UV CO_2 cell incubator was produced by Heraeus Holding GmbH (Hanau, Germany). The stereotactic apparatus was obtained from Zhenhua Bioinstrumentation LTD (Huaibei, China), and the SLY animal cerebral section mold was purchased from Suolinyuan Technology Company (Beijing, China). A freezing microtome was purchased from Leica Microsystems GmbH (Wetzlar, Germany). Mouse-anti-CNP-2',3'-cAMP-3'-phosphodiesterase (CNPase) monoclonal antibody, rabbit-anti-Nestin polyclonal antibody, rat-anti-CD68 monoclonal antibody and rabbit-anti-Ki67 monoclonal antibody were purchased from Abcam (Cambridge, UK). Mouse-anti-glial fibrillary acidic protein (GFAP) was purchased from BD Biosciences (Oxford, UK).

Labeling of C6 cells. C6 cells were cultivated in Dulbecco's modified Eagle's medium (DMEM)/F12, supplemented with 10% fetal calf serum (Gibco Life Technologies, Carlsbad, CA, USA) in 5% CO_2/95% air at 37˚C. Once the cells reached the logarithmic growth phase, the culture medium was removed, and the cells were washed twice with phosphate-buffered saline (PBS). Prior to labeling, CM-Dil was diluted in DMEM/F12 to a final concentration of 2 μM, and the C6 cells were incubated in this solution for 10 min at 37˚C, and 15 min at 4˚C. CM-Dil-stained cells (C6-CM-Dil) were washed with PBS three times and suspended in fresh culture medium. The SU3 human glioma cell line was transfected with the RFP gene using a lentivirus-mediated gene transfection kit (Genechem, Co., Ltd., Shanghai, China), according to the manufacturer's instructions.

Establishment of the dual-color orthotopic model of transplantable xenograft glioma. Transgenic female mice (BALB/c C57BL6J EGFP) expressing enhanced GFP (eGFP) were established in our laboratory (13), and cultivated in the Experiment Animals Center, Soochow University (Suzhou, China). The mice were used for research when they were aged 6-8 weeks and had a body weight of ~25 g. All of the mice were bred and maintained in the Specific Pathogen-Free Animal Care Facility. Following successful general anesthesia of the mice via intraperitoneal injection of 10% chloral hydrate (200 mg/kg), a small burr hole (2 mm in diameter) was made 2.5 mm right of the midline and 0.5 mm anterior to the bregma using a microskull drill, as outlined in Kaye *et al* (14). C6-CM-Dil and SU3-RFP ($1x10^5$) cells were injected into the right caudate nucleus at a depth of 3.5 mm, and a stereotactic apparatus assisted this procedure. The skull hole was then sealed with bone wax, and the scalps were sutured.

Dual-color tracing with whole-body in vivo fluorescence imaging of xenografts. The tumor-bearing mice were anesthetized by chloral hydrate injection (200 mg/kg) at 3, 5, 7, 9, 11, 13 and 15 days following tumor inoculation for *in vivo* fluorescent imaging using a live imaging system, with excitation and emission wavelengths of 470 and 535 nm for GFP, and 558 and 583 nm for RFP.

Generation of serial frozen tumor sections. Following completion of live imaging, the chests of the mice were opened under anesthesia, and 1-2 ml of normal saline was slowly injected into the left ventricle. A small incision was made on the auricle of the right atrium to allow blood to flow out. This step was immediately followed by the perfusion of 5-10 ml of 4% paraformaldehyde into the left ventricle. The whole brain was obtained and fixed in 4% formaldehyde for 7-8 h, following which it was dehydrated in a 20%, and then a 30%, sucrose solution. The brain was ready for coronal slicing upon sinking to the bottom of the sucrose solution, and this was performed using the SLY mold, by which continual, coronal cerebral sections of 1 mm thickness could be obtained (Fig. 1).

The third to sixth coronal sections (the location of the transplantation tumor) were embedded in optimal cutting temperature media, and continual tissue sections of 5 μm thickness were prepared using a freezing microtome. Subsequently, the sections were stained with DAPI (1 μg/ml), sealed with anti-fade mounting medium and stored at -20˚C. Routine hematoxylin and eosin (HE) staining and immunohistochemistry staining with antibodies against GFAP (1:400), 11-5bCNPase (1:600), CD68 (1:100), Nestin (1:400) and Ki67 (1:500), were performed for all slices.

Results

Whole-body in vivo fluorescence imaging of the xenografts. *In vivo* imaging of the xenografts was performed prior to pathological study at days 1, 3, 5, 7, 9, 11, 13 and 15, following inoculation of SU3-RFP and C6-CM-Dil cells into the right caudate nucleus. Dual-color images demonstrated that the tumor masses emitted red fluorescence from the corresponding inoculated site, and that the size of the tumors gradually increased over time (Fig 2). However, the tumors initiated by SU3-RFP cells grew at a slightly slower rate, as compared with the tumors consisting of C6-CM-Dil cells.

Anatomical location of xenografts with red fluorescence. The section containing the largest tumor was selected using

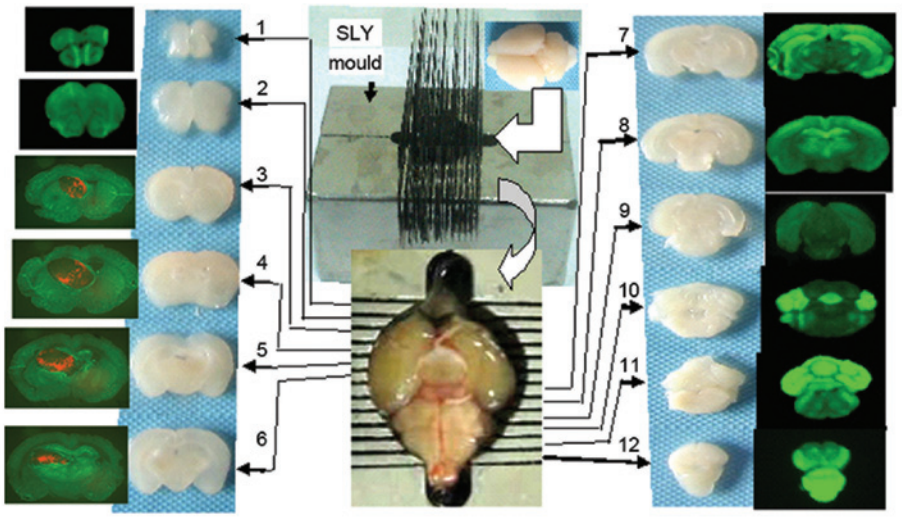

Figure 1. Frozen brain sections (1 mm, coronal) were produced using the SLY mold. Brains were placed into the SLY mold, and two section razors were placed in each crevice, after which continuous sections (1 mm thickness) were made by extracting the two razors from the nearby crevices. Sections 1-12 correspond to consecutive sections from the lobus olfactorius to the bulbus medullae.

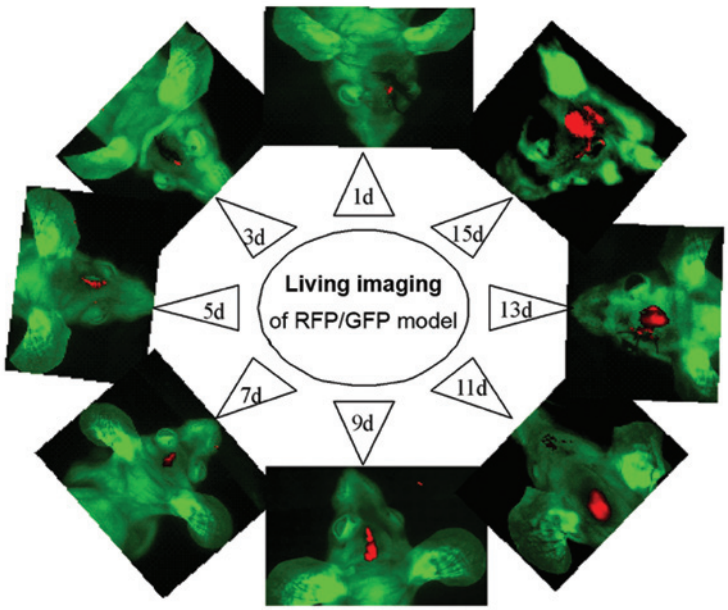

Figure 2. Dual-color tracing, whole-body, *in vivo* fluorescence imaging of the green fluorescent protein (GFP) in nude mice transplanted with tumors containing red fluorescent protein (RFP)-expressing rat C6 cells (C6-CM-Dil). The red fluorescence emitted by the tumor mass increased from 1-15 days following inoculation.

the SLY coronal mold, and the relative positions of the tumor and host tissues were detected using a fluorescence microscope. The exact position and size of the tumor was determined according to the Paxinos atlas (15). The stark contrast between the red fluorescence emitted by the transplanted tumor cells and the green fluorescence emitted by host tissues enabled the identification of even small tumor masses.

Histological characteristics of the transplanted tumor. C6-CM-Dil cells inoculated into the caudate nucleus were able to grow and easily migrate to the cerebral parenchyma, ventricles, choroid plexus, and subarachnoid cavity. The histological characteristics of the transplanted tumor resembled those of the host tissue where the tumor was located at that time, particularly in the choroid plexus (Fig. 3).

Invasion of tumor cells. SU3 cells expressing RFP were highly invasive, and were demonstrated to have migrated out and around the tumor in flocks, with some single cells being scattered away from the edge of the tumor where the host tissue appeared normal. Dual-color fluorescence permitted visualization of tumor cells invading the smooth muscle septum of the host vessel wall, which could not easily be identified in histological sections without fluorescence tracing (Fig.4).

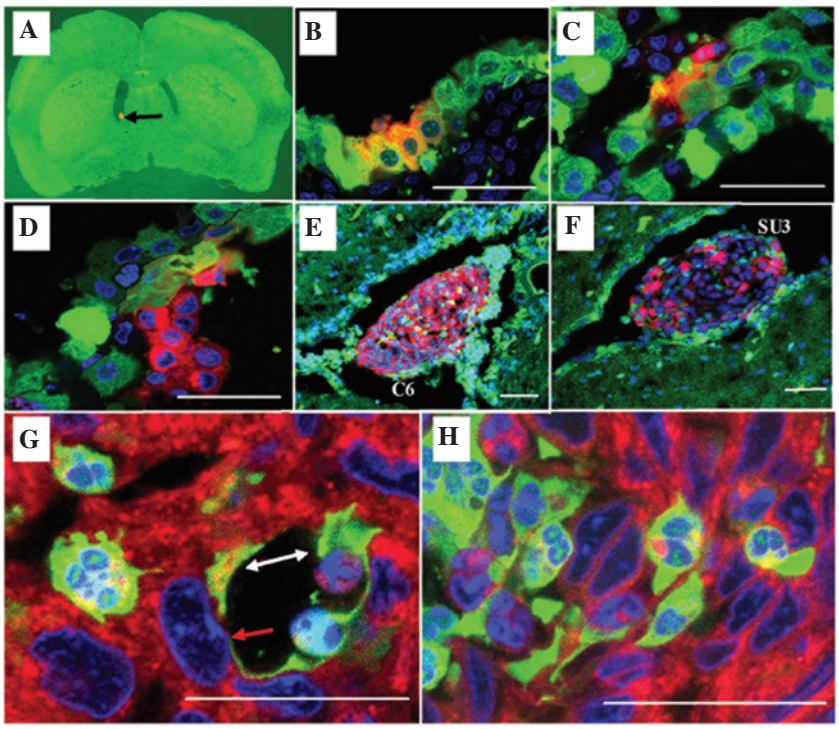

Figure 3. Choroid plexus papillary epithelioma was analyzed using laser confocal microscopy (scale 20 μm). Red fluorescent C6 or SU3 cells were injected into the lateral ventricle of a green fluorescent nude mouse with the assistance of stereotaxic apparatus: (A) Red fluorescent protein (RFP)-expressing tumor cells (black arrow; magnification, x12.5) settled at the lateral ventricle 1 day following implantation. (B and C) Cell fusions consisting of choroid corpora mammillaria cells and tumor cells 3 days following implantation; some of the choroid corpora mammillaria infrastructure remained (B) normal, whereas other parts were (C) disordered. (D) The tumor predominantly consisted of RFP-expressing tumor cells that projected into the cerebroventricular region 11 days following implantation. (E and F) At the advanced stage of the tumor 15 days following implantation, the tumor appeared large and was accompanied by hydrocephalus. (G and H) Although a few green fluorescent protein-expressing host cells were found in the tumor, the majority were fused polykaryocytes. In particular, mosaic blood vessels were formed by the tumor cells (white arrow; G), and fused host endothelial cells (red arrow; G) could be observed in the choroid plexus.

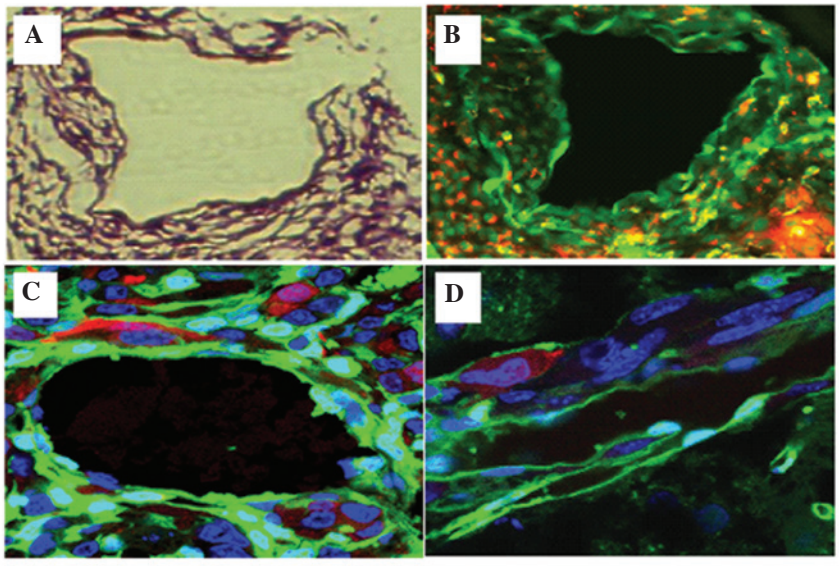

Figure 4. Visualization of tumor vessel formation in an SU3-red fluorescent protein (RFP) orthotopic transplantation tumor, in which red fluorescent tumor cells invaded into the host vessel wall (scale 50 μm): (A and B) RFP-expressing tumor cells invaded into the smooth muscle *spatium intermusculare* of the green fluorescent protein (GFP)-expressing host vessel wall; (C and D) visualization of RFP-expressing tumor cells transforming into vascular endothelial (white arrow, C) and pericyte-like cells (yellow arrow, C and D) using fluorescent scanning laser confocal microscopy within the tumor vessel area.

Blood vessels of xenografts. The transplanted tumor tissue was observed to possess numerous blood vessels. The origin of the cells in the tumor blood vessels could be distinguished by their fluorescence: Green cells from the host and red cells from the tumor. Yellow cells corresponded to fusions of tumor and host cells. Furthermore, fluorescence imaging permitted

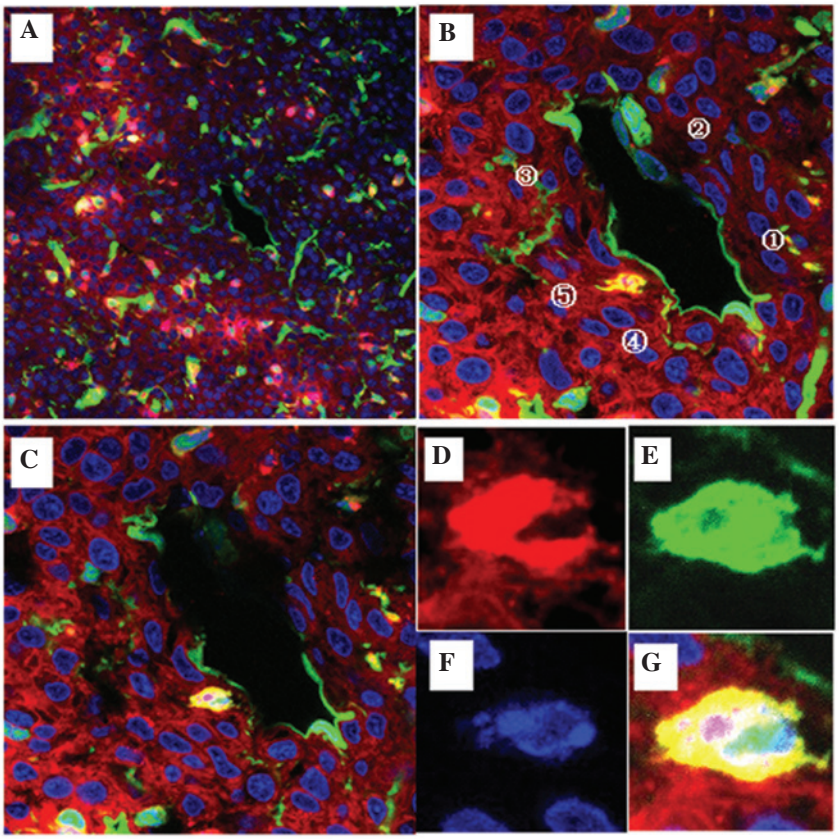

Figure 5. Visualization of mosaic blood vessels in the C6-CM-Dil orthotopic transplantation tumor using laser confocal microscopy (scale bar, 20 μm). (A) The red color corresponds to CM-Dil-stained tumor cells, the green color corresponds to green fluorescent protein (GFP)-expressing host tissue and cells, and the blue color corresponds to DAPI-staining in the nucleus. The borderline of the tumor was clear and the blood vessel section (white pane) is amplified in (B). (B and C) GFP was expressed throughout [1] the endomembrane and in [2] the majority of endothelial cells of the blood vessel. Some tumor cells were embedded in the blood vessel in [3] the absence of or [4] within an intact endomembrane. Examples of cell fusions [5] were observed in the deep tissue layers using tomographic scanning. (D-G) An amplified fused cell exhibited red, green, and blue fluorescence, suggesting that the cell was a fusion of a tumor cell and host vessel cell wall cell.

identification of the origins of the blood vessel endothelium, elastic fibers and perithelial cells of the vessel wall, which in turn demonstrated the occurrence of vascular mimicry.

Cell fusions between the transplanted tumor and host cells. Wherever the tumors grew, they consisted of red, green and yellow fluorescent cells. Although the number of yellow cells was fewer, as compared with the red and green cells, they could be found throughout the tumorigenesis and development processes. Under a fluorescence microscope, the SU3-RFP and C6-CM-Dil cells were red, whereas the host cells were green; therefore, the yellow cells corresponded to cellular fusions. These fused cells were detected wherever the tumor had migrated, including the choroid plexus (Fig. 3), tumor vessels (Fig. 4 and 5) and other cellular interstitialis of the tumor. Furthermore, laser confocal microscopy demonstrated that these fusions typically appeared within a portion of or within the entire cytoplasm and in the nucleolus (Fig. 6).

Tumor microenvironment imaging. The tumor microenvironment contains stromal cells and interstitial fluid, and mainly comprises the intratumoral and peripheral microenvironments. In conventional tumor histological sections, the tumor microenvironment cannot be easily studied due to the lack of a proper tracing method. However, the method used in the present study was able to distinguish the cellular origin of every cell in the tumor mass, and this was particularly important in areas containing few or no tumor cells. Furthermore as the tumor color and luster changed, sites where tumor cells were remodeling their microenvironment, which were called 'emergency reaction zones' in the present study, could be detected (Fig. 7).

Immunohistochemistry demonstrated the existence of cells strongly expressing the astrocyte marker protein GFAP, oligodendroglia marker protein CNPase, and Nestin (the marker of progenitors of astrocytes and oligodendroglia) in the emergency reaction zone tissue sections. This phenomenon suggested that neuralgia cells were forced to dedifferentiate into immature cells with upregulated expression of Ki-67 under physiopathological stress. Furthermore, the distribution of $CD68^+$ (marker protein of macrophage) cells suggests that immune-inflammatory cells reaching and surrounding the tumor reaction zone may participate in the physiopathological process (Fig. 8).

Discussion

Prior to the 1960s, non-immunodeficient mice or rats were widely used as brain tumor models, and were transformed using carcinogenic agents, including chemical materials and a virus.

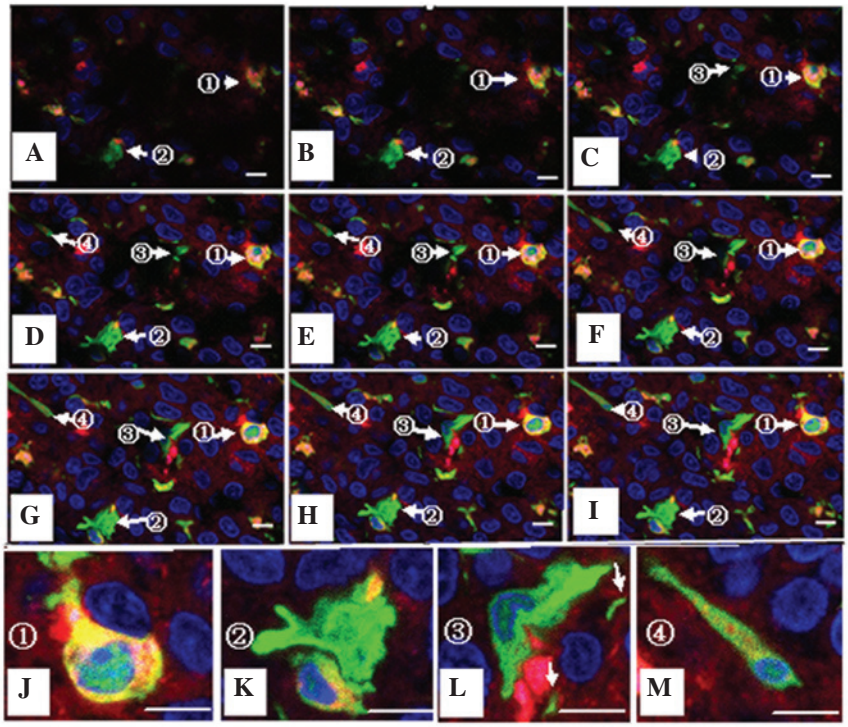

Figure 6. Visualization of cell fusion in an SU3-RFP orthotopic transplantation tumor using fluorescence tomographic scanning (section thickness, 20 μm) and laser confocal microscopy. The tumor cells, host cells, karyon and fused cells are red, green, blue and yellow, respectively. (A-I) Four fusion cells with various morphologies were observed in 9 sections according to DAPI staining. (J-M) correspond to amplified portions of (I): (J) Cell 1, which was entirely fused with another cell, was round, with a central nucleus and a predominantly yellow cytoplasm; (K) cell 2 was a green cell with a stretched out parapodium, as if attempting to phagocytose the adjacent yellow cell; (L) cell 3 was a green cell that was being put under pressure by an adjacent red cell, with green-cell derived debris apparent (white arrow); and (M) cell 4 was a long fusiform with an eccentric nucleus, which contained large red granules and small green/yellow granules in the cytoplasm.

Due to the appearance of immunodeficient nude mice and severe combined immunodeficiency mice in the 1960s, various types of human tumor xenograft models were successfully established, which greatly promoted the *in vivo* study of oncogenicity and the experimental effectiveness of human cancer (16-18). At that time, researchers typically used changes in the size of a tumor as an indicator of effectiveness; however, describing the precise anatomical location of tumors was challenging. The method used in the present study permitted easy identification of the anatomical location of a tumor and allowed the study of the tumor microenvironment. Charles *et al* (1) reported that a number of cells in the tumor microenvironment were recruited from the host bone marrow or circulation, and had little association with the anatomic site of the tumor. However, the use of traditional models may result in some errors, including when determining cell origin using HE staining, immunohistochemistry and even immunofluorescence tracing.

The long, carbon-chain carbocyanine dye CM-Dil that was used in the present study is lipid-soluble, and therefore becomes incorporated into the plasma membrane. CM-Dil does not affect the survival, development or basic physiological properties of the labeled cells, and does not detectably spread from labeled to unlabeled cells (19). As compared with RFP, CM-Dil is not integrated into the cell chromosome and may be lost during cell passaging. However, in a previous study, cells could be traced *in vitro* and *in vivo* for up to six weeks following CM-Dil labeling, and the process of CM-Dil labeling was convenient and fast (20).

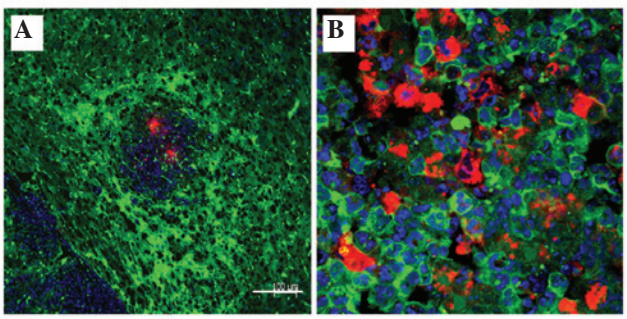

Figure 7. Tumor microenvironment of a C6-CM-Dil orthotopic transplantation tumor using laser confocal microscopy. (A) In the primary stages of the xenograft, the host cells and tumor tissue developed an intensive emergency reaction, which was demonstrated by green color, as compared with the outer normal tissue, although the red tumor was still small (scale bar, 100 μm). (B) Within the tumor itself, the number of tumor cells nearly equaled the number of green host cells (scale bar, 200 μm).

It is important to investigate every component of the tumor microenvironment. All interstitial cells, with the exception of transplanted tumor cells and their daughter cells, are members of the tumor microenvironment, including host cells surrounding tumor transplantation sites and host cells that migrate to the site from the vicinity or from distant sites. When using histological sections of traditional animal models it is often difficult to distinguish between tumor and host cells. However, the dual-color fluorescence-tracing glioma model used in the present study allowed easy observation and

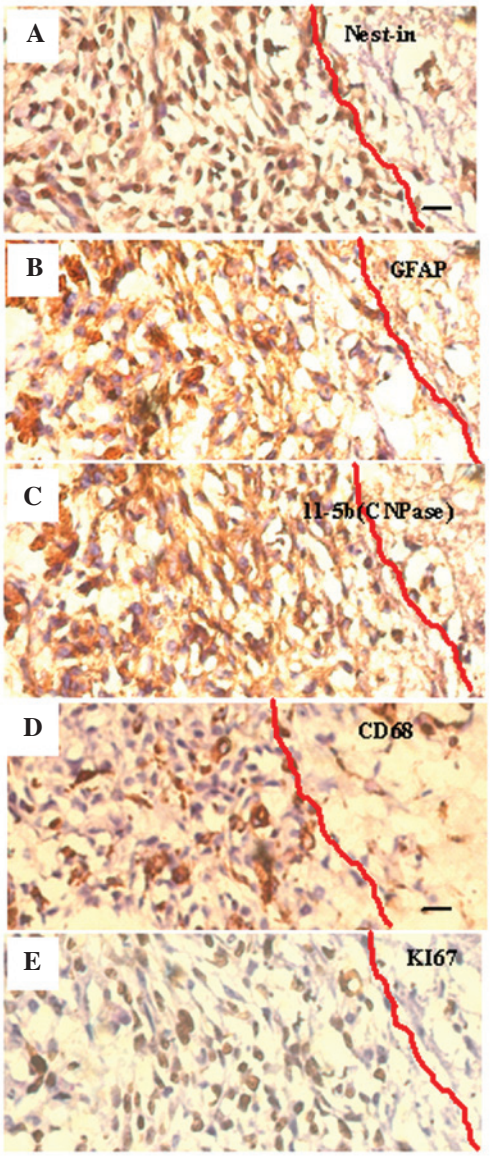

Figure 8. Identification of the cell (SU3) type via visualization of protein markers in the stress reaction zone surrounding the tumor (immunohistochemistry dyeing from contiguous slices of the same specimen; scale bar, 20 μm): (A) Nestin, expressed predominantly in the cytoplasm (brown immunocomplex), identified neuroglia precursor cells; (B and C) astrocyte-related glial fibrillary acidic protein (GFAP, B) and oligodendrocyte-related phosphodiesterase (CNPase, C) were expressed in the cytoplasm of some of the cells (brown immunocomplex); (D) Monocyte/macrophage associated CD68$^+$ cells distributed in the reaction zone between cells (brown immunocomplexes); (E) the proliferation cell nuclear antigen Ki67 (brown immunocomplex expressed in karyons)-positive cells formed ~80% of all cells, and this suggested that the majority of cells were undergoing proliferation, regardless of the numerous cellular types.

discrimination of these cells, based on the color of their fluorescence: Red for transplanted tumor-derived cells and green for host-derived cells.

The dual-color fluorescence-tracing glioma model facilitated the study of the tumor microenvironment by enabling easy discrimination between tumor- and host-derived cells, and permitting visualization of invading tumor cells, including their remodeling of the host environment. Therefore, the present study was able to identify the part of the host that was under pressure from tumor remodeling, based on the precise location of the tumor cell in SLY brain sections of this model.

In dual-color fluorescence tracing sections, yellow fluorescent cells, which were expressing both RFP and GFP, and which can not be easily identified using traditional tumor models, corresponded to fusion cells of the RFP-expressing tumor cells and GFP-expressing host cells. It has been suggested that multinucleated giant cells are fused cells, although fused cells are not necessarily multinucleated giant cells. Cell fusion has a crucial function in the genesis and development of a tumor (21-28), as the daughter cells of the fusion cells may become immature cells by retrodifferentiation or transdifferentiation into other blastodermic cells. These observations have aided progress in the study of tumor angiogenesis, tumor-associated cell carcinogenesis, tumor cell heterogeneity and tumor cell remodeling of the microenvironment, which is induced by tumor stem/progenitor cells. The results of the present study demonstrated that tumor cells were able to fuse with various types of cells within their microenvironment, including gitter, vascular endothelial, vascular smooth muscle and choroid plexus papillary cells.

Controversy remains with regards to the transdifferentiation of glioma stem/progenitor cells into vascular endothelial cells. Cheng *et al* (29) suggested that tumor cells may transdifferentiate into pericytes but not into endothelial cells. However, the results of the present study suggested that tumor-derived RFP-expressing cells were able to transform into both endothelial and perithelial cells.

In conclusion, the present study identified the presence of red, green and yellow fluorescent cells in the vessel walls of the neoformative vascular region, although their proportion dynamically changed over time, particularly the number of yellow, fusion cells. Future studies should endeavor to culture yellow cells from the transplantation tumor and assess their differentiation direction towards endothelial and/or perithelial cells by analyzing their marker proteins.

Acknowledgements

This study was supported by grants from the National Natural Science Foundation of China (grant nos. 81071766, 81172400, 81272799, 81272793, and 81101909) and the Jiangsu Provincial Special Program of Clinical Medical Science (no. BL2014040), Suzhou Science and Technology Development Program (nos. SYS201269, SYSD2013087 and SZS201509).

References

1. Charles NA, Holland EC, Gilbertson R, Glass R and Kettenmann H: The brain tumor microenvironment. Glia 60: 502-514, 2012.
2. Dong J, Zhang Q, Huang Q, Chen H, Shen Y, Fei X, Zhang T, Diao Y, Wu Z, Qin Z, *et al*: Glioma stem cells involved in tumor tissue remodeling in a xenograft model. J Neurosurg 113: 249-260, 2010.
3. Dong J, Zhao Y, Huang Q, Fei X, Diao Y, Shen Y, Xiao H, Zhang T, Lan Q and Gu X: Glioma stem/progenitor cells contribute to neovascularization via transdifferentiation. Stem Cell Rev 7: 141-152, 2011.
4. Paget S: The distribution of secondary growths in cancer of the breast. 1889. Cancer Metastasis Rev 8: 98-101, 1989.
5. Fidler IJ: Seed and soil revisited: Contribution of the organ microenvironment to cancer metastasis. Surg Oncol Clin N Am 10: 257-269, vii-viii, 2001.

6. Fidler IJ: The organ microenvironment and cancer metastasis. Differentiation 70: 498-505, 2002.
7. Fidler IJ: The pathogenesis of cancer metastasis: The 'seed and soil' hypothesis revisited. Nat Rev Cancer 3: 453-458, 2003.
8. Hayashi K, Kimura H, Yamauchi K, Yamamoto N, Tsuchiya H, Tomita K, Kishimoto H, Hasegawa A, Bouvet M and Hoffman RM: Comparison of cancer-cell seeding, viability and deformation in the lung, muscle and liver, visualized by subcellular real-time imaging in the live mouse. Anticancer Res 31: 3665-3672, 2011.
9. Suetsugu A, Katz M, Fleming J, Truty M, Thomas R, Saji S, Moriwaki H, Bouvet M and Hoffman RM: Non-invasive fluorescent-protein imaging of orthotopic pancreatic-cancer-patient tumorgraft progression in nude mice. Anticancer Res 32: 3063-3067, 2012.
10. Bouvet M and Hoffman RM: In vivo imaging of pancreatic cancer with fluorescent proteins in mouse models. Methods Mol Biol 872: 51-67, 2012.
11. Menen RS, Hassanein MK, Momiyama M, Suetsugu A, Moossa AR, Hoffman RM and Bouvet M: Tumor-educated macrophages promote tumor growth and peritoneal metastasis in an orthotopic nude mouse model of human pancreatic cancer. In Vivo 26: 565-569, 2012.
12. Dong J, Dai XL, Lu ZH, Fei XF, Chen H, Zhang QB, Zhao YD, Wang ZM, Wang AD, Lan Q and Huang Q: Incubation and application of transgenic green fluorescent nude mice in visualization studies on glioma tissue remodeling. Chin Med J (Engl) 125: 4349-4354, 2012.
13. Wu ZC, Huang Q, Shao YX, Xue ZM, Dong J, Diao Y, Wang AD and Lan Q: Transplantation of human glioma stem cells in nude mice with green fluorescent protein expression. Zhonghua Yi Xue Za Zhi 88: 2317-2320, 2008. (In Chinese)
14. Kaye AH, Morstyn G, Gardner I and Pyke K: Development of a xenograft glioma model in mouse brain. Cancer Res 46: 1367-1373, 1986.
15. Paxinos G and Franklin KBJ: The Mouse Brain in Stereotaxic Coordinates. 2nd edition. Academic Press, San Diego, 2001.
16. Rana MW, Pinkerton H, Thornton H and Nagy D: Heterotransplantation of human glioblastoma multiforme and meningioma to nude mice. Proc Soc Exp Biol Med 155: 85-88, 1977.
17. Fei XF, Zhang QB, Dong J, Diao Y, Wang ZM, Li RJ, Wu ZC, Wang AD, Lan Q, Zhang SM and Huang Q: Development of clinically relevant orthotopic xenograft mouse model of metastatic lung cancer and glioblastoma through surgical tumor tissues injection with trocar. J Exp Clin Cancer Res 29: 84, 2010.
18. Chen H, Dong J and Huang Q: Xenograft model of human brain tumor. In: Brain Tumors: Current and Emerging Therapeutic Strategies. Abujamra AL (ed). InTech, Shanghai, China, pp3-20, 2011.
19. Honig MG and Hume RI: Fluorescent carbocyanine dyes allow living neurons of identified origin to be studied in long-term cultures. J Cell Biol 103: 171-187, 1986.
20. Weir C, Morel-Kopp MC, Gill A, Tinworth K, Ladd L, Hunyor SN and Ward C: Mesenchymal stem cells: Isolation, characterisation and in vivo fluorescent dye tracking. Heart Lung Circ 17: 395-403, 2008.
21. He X, Tsang TC, Pipes BL, Ablin RJ and Harris DT: A stem cell fusion model of carcinogenesis. J Exp Ther Oncol 5: 101-109, 2005.
22. Shinn-Thomas JH, Scranton VL and Mohler WA: Quantitative assays for cell fusion. Methods Mol Biol 475: 347-361, 2008.
23. Dittmar T, Nagler C, Schwitalla S, Reith G, Niggemann B and Zänker KS: Recurrence cancer stem cells - made by cell fusion? Med Hypotheses 73: 542-547, 2009.
24. Lu X and Kang Y: Cell fusion hypothesis of the cancer stem cell. Adv Exp Med Biol 714:129-140, 2011.
25. Nagler C, Zänker KS and Dittmar T: Cell fusion, drug resistance and recurrence CSCs. Adv Exp Med Biol 714: 173-182, 2011.
26. Goldenberg DM: Horizontal transmission of malignancy by cell-cell fusion. Expert Opin Biol Ther 12 (Suppl 1): S133-S139, 2012.
27. Parris GE: Historical perspective of cell-cell fusion in cancer initiation and progression. Crit Rev Oncog 18: 1-18, 2013.
28. Harkness T, Weaver BA, Alexander CM and Ogle BM: Cell fusion in tumor development: Accelerated genetic evolution. Crit Rev Oncog 18: 19-42, 2013.
29. Cheng L, Huang Z, Zhou W, Wu Q, Donnola S, Liu JK, Fang X, Sloan AE, Mao Y, Lathia JD, *et al*: Glioblastoma stem cells generate vascular pericytes to support vessel function and tumor growth. Cell 153: 139-152, 2013.